

ORIGINAL ARTICLE

Alcohol dehydrogenase 5 of *Helicoverpa armigera* interacts with the *CYP6B6* promoter in response to 2-tridecanoneJie Zhao^{1,2} , Qian Wei¹, Xin-Rong Gu¹, Su-Wei Ren¹ and Xiao-Ning Liu¹

¹Xinjiang Key Laboratory of Biological Resources and Genetic Engineering, College of Life Sciences and Technology, Xinjiang University, Urumqi, Xinjiang, China and ²Key Laboratory of Oasis Agricultural Pest Management and Plant Protection Resources Utilization, College of Agriculture, Shihezi University, Shihezi, Xinjiang, China

Abstract Alcohol dehydrogenase 5 (ADH5) is a member of medium-chain dehydrogenase/reductase family and takes part in cellular formaldehyde and S-nitrosoglutathione metabolic network. 2-tridecanone (2-TD) is a toxic compound in many *Solanaceae* crops to defend against a variety of herbivory insects. In the broader context of insect development and pest control strategies, this study investigates how a new ADH5 from *Helicoverpa armigera* (*HaADH5*) regulates the expression of *CYP6B6*, a gene involved in molting and metamorphosis, in response to 2-TD treatment. Cloning of the *HaADH5* complementary DNA sequence revealed that its 1002 bp open reading frame encodes 334 amino acids with a predicted molecular weight of 36.5 kD. *HaADH5* protein was purified in the *Escherichia coli* Transetta (pET32a-*HaADH5*) strain using a prokaryotic expression system. The ability of *HaADH5* protein to interact with the 2-TD responsive region within the promoter of *CYP6B6* was confirmed by an *in vitro* electrophoretic mobility shift assay and transcription activity validation in yeast. Finally, the expression levels of both *HaADH5* and *CYP6B6* were found to be significantly decreased in the midgut of 6th instar larvae after 48 h of treatment with 10 mg/g 2-TD artificial diet. These results indicate that upon 2-TD treatment of cotton bollworm, *HaADH5* regulates the expression of *CYP6B6* by interacting with its promoter. As *HaADH5* regulation of *CYP6B6* expression may contribute to the larval xenobiotic detoxification, molting and metamorphosis, *HaADH5* is a candidate target for controlling the growth and development of cotton bollworm.

Key words alcohol dehydrogenase; DNA-protein interaction; *Helicoverpa armigera*; regulatory factor; 2-tridecanone

Introduction

Alcohol dehydrogenases (ADHs) of medium-chain dehydrogenase/reductase (MDR) superfamily play important roles in many physiological processes, including the metabolism of ethanol, aldehydes, steroids, retinoids, lipid peroxidation products, hydroxy fatty acids, and xenobiotic

alcohols (Ramchandani *et al.*, 2001; Oscar & Marinkovic, 2003; Luo *et al.*, 2008; Chase *et al.*, 2009; Anand *et al.*, 2014).

ADH5 belongs to the MDR family and functions as a homodimer that localizes to the nucleus and cytoplasm (Yang *et al.*, 1997; Fernández *et al.*, 2003). Each subunit of the homodimer has two tightly bound zinc atoms, the one catalytic zinc at the active site and the other structural zinc in a lobe of the catalytic domain (Kaiser *et al.*, 1988; Östberg *et al.*, 2016). ADH5 does not normally metabolize ethanol, aldehydes or retinoids, and it was identical to formaldehyde dehydrogenase and S-nitrosoglutathione reductase based on its amino acid sequence and its

Correspondence: Xiao-Ning Liu, Xinjiang Key Laboratory of Biological Resources and Genetic Engineering, College of Life Sciences and Technology, Xinjiang University, Urumqi 830046, China. Fax: +86 991 8582076; email: liuxn0103@sina.com

structural and kinetic properties (Koivusalo *et al.*, 1989; Jensen *et al.*, 1998; Deltour *et al.*, 1999).

The characterization of ADH5 has focused on its functions in the formaldehyde and nitrogen oxide metabolism pathways. Formaldehyde can rapidly attack electron-rich thiol and amino groups to form covalent adducts, such as DNA interstrand crosslinks and DNA-protein crosslinks; the resulting blockage of transcription and replication can lead to mutagenesis and cell death (Kawanishi *et al.*, 2014). ADH5 plays a central role in formaldehyde metabolism to prevent cytotoxicity and provides one carbon unit for nucleotide biosynthesis (Tibbetts & Appling, 2010; Pontel *et al.*, 2015; Burgos *et al.*, 2017). ADH5 can also convert S-nitrosoglutathione, a stable nitrogen oxide reserve, to S-nitrosothiol, resulting in the post-translational S-nitrosylation of a protein at the same time (Wei *et al.*, 2010; Smith & Marletta, 2012; Corti *et al.*, 2014). The S-nitrosylation protein modification is a potential signal in physiological processes, such as the generation of cyclic guanosine monophosphate, inactivation of certain enzymes to cause DNA damage, and inhibition or induction of apoptotic cell death (Hess *et al.*, 2005; Martínez *et al.*, 2011).

The ADH5 of insects was first found in several *Drosophila* species with 70% identity to the corresponding human form and was highly selective for formaldehyde rather than ethanol, its enzymatic property being compatible with the constitutive nature of the homolog in vertebrates (Danielsson *et al.*, 1994). In the past two decades, little research on ADH5 has been done in insects. The expression and activity of ADH5 was significantly changed as a metabolizing enzyme in response to toxic industrial additives and heavy metals in larvae of *Chironomus riparius* (Park & Kwak, 2009a, 2009b). Then, ADH5 was confirmed to play a critical role in degradation of odorants and xenobiotics as a biotransformation enzyme within antennae of *Cydia pomonella* (Huang *et al.*, 2016). In recent years, thanks to the rapid development of transcriptome, more and more ADH5 was found and suggested to participate in the metamorphosis and pheromone chemosensory system in a lot of insects. The transcriptome displayed ADH5 present in wing discs during the larva-to-pupa metamorphosis and might be involved in chitin biosynthesis of *Bombyx mori* (Ou *et al.*, 2014). The transcriptomic analysis of the female sex pheromone glands showed ADH5 could be involved in sex pheromone biosynthesis and degradation pathways in diamondback moth, black cutworm and three noctuid moths (Vogel *et al.*, 2010; Gu *et al.*, 2013; Li *et al.*, 2015; He *et al.*, 2017).

Helicoverpa armigera (Lepidoptera: Noctuidae) seriously impacts the output of many agricultural and

economic crops. Meanwhile, these plants could synthesize a variety of toxic substances to defend against this herbivory pest. 2-tridecanone (2-TD) is an important secondary substance in Solanaceae plants. Its concentration in leaves can be as high as 0.39%, which can induce excessive expression of various insect cytochrome P450 genes including *CYP6B6* (Yu *et al.*, 2002; Liu *et al.*, 2006). *CYP6B6* is important for the detoxification of exogenous toxic substances, growth, and developmental process in cotton bollworm (Zhao *et al.*, 2016a). In previous research, we identified a 2-TD responsive region in the *CYP6B6* promoter, designated as the HE1 element, using transient transfection and mobility shift assays (Li *et al.*, 2014). Using the yeast one-hybrid method, we subsequently identified candidate regulators that bind to the *CYP6B6* HE1 element, and one of these was found to be a previously uncharacterized ADH5 of *H. armigera* (*HaADH5*) based on the results of National Center for Biotechnology Information Basic Local Alignment Search Tool (NCBI BLAST) analysis.

The functions of insect ADH5 in growth and developmental processes have not been clearly confirmed in the available literature. To investigate whether *HaADH5* regulates the expression of *CYP6B6* upon treatment with the toxic substance 2-TD, we cloned the *HaADH5* complementary DNA (cDNA) sequence using rapid amplification of cDNA ends (RACE) and also tested the interaction between *HaADH5* protein and the *CYP6B6* HE1 element through an *in vitro* electrophoretic mobility shift assay and transcription activity validation in yeast. Using real-time quantitative polymerase chain reaction (PCR) and Western blotting, *HaADH5* and *CYP6B6* expression were also detected in the midgut of 6th instar larvae exposed to 2-TD. The present findings demonstrate the broader range of ADH5 function as a regulatory factor affecting the expression of a gene involved in detoxification, metabolism, growth, and development in cotton bollworm.

Materials and methods

Insects

The cotton bollworm population used in this study (a laboratory population) was initially collected from the Anningqu town of Urumqi in Xinjiang Autonomous Region, China, and reared on an artificial diet in a growth room maintained at 26 ± 1 °C, 70%–80% relative humidity, with a photoperiod of 16 : 8 h (L : D). The population was never exposed to any pesticides. The composition of the artificial diet was as follows: corn flour 300 g, soybean powder 100 g, yeast extract powder 100 g, citric acid 2.5 g,

vitamin C 10 g, sorbic acid 1.5 g, vitamin B 1.5 g, erythromycin 0.05 g, propionic acid 5 mL, vitamin E 1.5 g, water 2.5 L.

Plasmids, antisera, and bacterial and yeast strains

The pMD18-T, pET32a, and pGADT7 vectors were purchased from Takara Bio, EMD Biosciences, and Clontech, respectively. The polyclonal antisera of anti-CYP6B6, anti- β -Actin, and anti-HaADH5 were prepared by our research group (Huang *et al.*, 2015; Wei *et al.*, 2015). Competent cells of *Escherichia coli* strains DH5 α and Transetta were purchased from TransGen Biotech. The yeast strains Y1HGold (p4r-AbAi) and Y1HGold (p4m-AbAi) were constructed by our research group as previously reported (Zhao *et al.*, 2016b).

HaADH5 sequencing by RACE

Total RNA was extracted from the midgut of 6th instar larvae using the TansZol Up Plus RNA Kit (TransGen Biotech, Beijing, China) then reverse transcribed into RACE-Ready cDNA using the SMARTer RACE 5'/3' Kit (Clontech Laboratories, Mountain View, CA, USA).

Based on the nucleotide sequence determined by yeast one-hybrid screening, we designed primers for RACE amplification of *HaADH5* by DNAMAN software (Table 1). The outer PCR reaction conditions were 94 °C for 5 min, followed by 94 °C for 30 s, 68 °C for 30 s, and 72 °C for 3 min (25 cycles). The outer PCR product was diluted 50-fold then used as the template for the inner PCR reaction. The inner PCR conditions were 94 °C for 5 min, followed by 94 °C for 30 s, 58 °C for 30 s, and 72 °C for 3 min (30 cycles). After the inner PCR amplification, the product was recycled, ligated into pMD18-T vector, and transformed into *E. coli* DH5 α . Positive clones were identified by bacterial solution PCR detection and sent for sequencing (Sangon Biotech, Shanghai, China). Using DNAMAN software, the 5' and 3' end sequences were assembled to obtain the cDNA sequence of *HaADH5*, and its open reading frame (ORF) was predicted using ORF Finder tool in the NCBI database.

The conserved amino acid of *HaADH5* was analyzed by Protein BLAST in the NCBI database. The phylogenetic tree of *HaADH5* was constructed by neighbor-joining analyses using MEGA software with 1000 replicates of bootstrap values. The secondary structure of *HaADH5* was predicted including signal peptide, transmembrane domain and subcellular localization by SignalP, TMHMM and TargetP tools of CBS Prediction Servers software,

then its tertiary structure was predicted using SWISS-MODEL software and Protein Data Bank (PDB) database.

Expression and purification of HaADH5 protein in *E. coli*

The *HaADH5* ORF was amplified using the following reaction conditions: 94 °C for 5 min; 35 cycles of 94 °C for 30 s, 58 °C for 30 s, and 72 °C for 1 min; and 72 °C for 7 min. The purified PCR product was digested with *Kpn* I and *Not* I and ligated into the pET32a vector linearized with the same enzymes, followed by transformation into *E. coli* DH5 α competent cells (Cycle Pure Kit, Gel Extraction Kit, Plasmid Mini Kit, OMEGA Bio-tek, Norcross, GA, USA). After double enzyme digestion to ensure the insertion, pET32a-*HaADH5* was transformed into the *E. coli* Transetta strain for protein expression. The Transetta (pET32a-*HaADH5*) strain was incubated in lysogeny broth (LB) medium at 37 °C until the optical density at 600 nm reached 0.5. Isopropyl β -D-1-thiogalactopyranoside (IPTG) was added into the culture broth to a final concentration of 0.5 mmol/L. The culture was subsequently incubated at 20 °C for 4 h and collected by centrifugation at 7104 g at 4 °C (Ai *et al.*, 2017).

For purification of the His-*HaADH5* protein, cell pellets from 1 L of induced culture broth were completely suspended in phosphate-buffered saline (PBS, pH 7.0) by gently vortexing. The cell suspension was sonicated for 15 min with 5 s bursts alternated with chilling on ice to decrease viscosity, followed by centrifugation at 15 984 g for 10 min at 4 °C. The supernatant was directly loaded onto a 2 mL column of Ni²⁺-NTA His Bind Resins (Novagen, Madison, WI, USA) equilibrated with Ni²⁺-NTA Binding Buffer. The settled resin was washed with wash buffer (300 mmol/L NaCl, 50 mmol/L NaH₂PO₄, pH 8.0) containing 5 mmol/L imidazole then eluted with a linear gradient of imidazole (10, 10, 20, 20, 50, 100, 200, 200 mmol/L). All protein purification steps were performed at 4 °C. All collected outflows were separated by 12% SDS-PAGE and stained with Coomassie blue.

The concentration and purity of His-*HaADH5* protein was tested using the Pierce Bicinchoninic Acid (BCA) Protein Assay Kit (Thermo Scientific, Waltham, MA, USA) and Western blotting. The protein was transferred onto a nitrocellulose (NC) membrane using the electrode diverting method. The NC membrane incubation steps were as follows: blocking buffer (PBS containing 3% defatted milk powder) for 1 h at 37 °C, anti-His-tag mouse monoclonal antibody in blocking buffer for 2 h at 37 °C, and peroxidase-conjugated goat anti-mouse

Table 1 Primers used in this study.

| Primer | Sequence (5' to 3') | Purpose |
|--------------------|---|--|
| 5'-outer | CTAATACGACTCACTATAGGGCAAGCAGTGGTA TCAACGCAGAGT | <i>HaADH5</i> 5' RACE outer PCR |
| 5'-P1 | TCATCCAACGCCACACAAGG | |
| 5'-inner | CTAATACGACTCACTATAGGGC | <i>HaADH5</i> 5' RACE inner PCR |
| 5'-P2 | GCAGGTTGTAGGATAGGTGCCTTGGG | |
| 3'-outer | TACCGTCGTTCCTACTAGTGATTT | <i>HaADH5</i> 3' RACE outer PCR |
| 3'-P1 | CTATCATCGATCCCAACGACAAAA | |
| 3'-inner | CGCGGATCCTCCACTAGTGATTTCACTATAGG | <i>HaADH5</i> 3' RACE inner PCR |
| 3'-P2 | TTGTCAGCCCAAAGCAGGT | |
| <i>HaADH5</i> -F | GAGGTACCATGGTGAAGGCACGGAAA, <i>Kpn</i> I | <i>HaADH5</i> ORF amplification for ligation into pET32a |
| <i>HaADH5</i> -R | GCGTCGACTTATAATTTAACAACAGCCT, <i>Sal</i> I | |
| <i>HaADH5</i> -yF | CCATATGATGGTGAAGGCACGGAAATA, <i>Nde</i> I | <i>HaADH5</i> ORF amplification for ligation into pGADT7 |
| <i>HaADH5</i> -yR | CCTCGAGTTATAATTTAACAACAGCCTTTC, <i>Xho</i> I | |
| β -Actin-QF | CACACCTTCTACAACGAGCTG | qPCR of target and reference genes |
| β -Actin-QR | GAGGATCTTCATGAGGTAGTCG | |
| <i>Tubulin</i> -QF | TCCAACCTCACACTCGCT | |
| <i>Tubulin</i> -QR | GGAAGCAGATGTCGTATAATG | |
| <i>HaADH5</i> -QF | GTCTCCGCGGCGCTCAA | |
| <i>HaADH5</i> -QR | TCATCCAACGCCACACAAGG | |
| <i>CYP6B6</i> -QF | TTCAAACCTTATACCATGTCCACAAT | |
| <i>CYP6B6</i> -QR | CCAATTGACGGAGCTCTAGAATCA | |

PCR, polymerase chain reaction; RACE, rapid amplification of complementary DNA ends; ORF, open reading frame.

immunoglobulin G (IgG) (H+L) for 2 h at 37 °C. After each incubation step, the membrane was washed with PBS three times. Finally, the membrane was stained with chemiluminescent substrate for 10 min using the BeyoECL Plus kit (Beyotime, Shanghai, China). The membrane was viewed using an ImageQuant LAS4000 imager (Fujifilm, Japan).

In vitro detection of *HaADH5* interaction with the *CYP6B6* promoter

The *CYP6B6* HE1 element was prepared as the DNA probe for the electrophoretic mobility shift assay (EMSA). The negative control contained only HE1 probe without *HaADH5* protein. For specific competition, excess unlabeled HE1 DNA was added. For non-specific competition, a 300 bp non-correlated sequence was added and denoted as bHLH that was a basic helix-loop-helix gene from *Chenopodium glaucum*. The EMSA/Gel-shift kit (Beyotime) was used for the reaction. Protein-bound probes were separated from free probes on 6% (w/v) non-denaturing PAGE in Tris-borate ethylenediaminetetraacetic acid buffer. All DNA bands were transferred onto Amersham Hybond-N⁺ Membrane (GE Healthcare,

Waukesha, WI, USA) using the electrode diverting method. DNA probe labeling and subsequent color detection were performed using the DIG High Prime DNA Labeling and Detection Starter Kit II (Roche, Basel, Switzerland) according to the manufacturer's protocol. Finally, the membrane was detected using an ImageQuant LAS4000 imager.

Validation of *HaADH5* interaction with the *CYP6B6* promoter in yeast

The reaction conditions for amplification of the *HaADH5* ORF were 94 °C for 5 min; 35 cycles of 94 °C for 30 s, 59 °C for 30 s, and 72 °C for 1 min; and 72 °C for 7 min. The purified PCR product was digested with *Nde* I and *Xho* I then ligated into pGADT7 vector linearized with the same enzymes. The pGADT7-*HaADH5* plasmid was transformed into the Y1HGOLD (p4r-AbAi) strain with the 2-TD responsive region of the *CYP6B6* promoter and into a mutant Y1HGOLD (p4m-AbAi) strain. The two strains were subsequently coated onto SD/-Leu medium with or without 100 ng/mL Aureobasidin A (AbA). In this analysis, if *HaADH5* interacted with the 2-TD responsive region of *CYP6B6*, the *AbA*^r reporter gene

would be active in the Y1HGold (p4r-AbAi) strain but not active in the Y1HGold (p4m-AbAi) strain.

HaADH5 and CYP6B6 expression in the midgut of H. armigera exposed to 2-TD

The newly molted 6th instar larvae, after molting for 1 day, were treated by 4 h of starvation treatment, then the larvae were exposed to the artificial diet mixed with 2-TD (Sigma-Aldrich, St Louis, MO, USA) (99% purity) 0 or 10 mg/g (w:w) for 6, 12, 20, 30, and 48 h. Each treatment contained 100 larvae. The tested larvae were starved for 30 min to defecate after the different feeding times. The midgut tissue was isolated from the experimental larvae on ice, cleaned in sterile water, then frozen in liquid nitrogen. Each sample contained three midgut tissues, and each group contained three samples.

Total RNA was extracted using the TansZol Up Plus RNA Kit, followed by cDNA synthesis using Reverse Transcriptase Moloney Murine Leukemia Virus (RNase H⁻) (TaKaRa, Kusatsu, Japan). The reaction setup and quantitative PCR (qPCR) cycling conditions were based on the protocol for the QuantiNova SYBR Green PCR kit (Qiagen, Germantown, MD, USA). The *β-Actin* and *Tubulin* genes were used to normalize the expression levels of the target genes among samples (Vandesompele *et al.*, 2002; Chandra *et al.*, 2014; Shakeel *et al.*, 2015). qPCR was performed in triplicate for each cDNA sample. All of the primer sets are listed in Table 1. The relative expression levels of the target genes were calculated using the $2^{-\Delta\Delta C_T}$ method. Using GraphPad Prism 5, one-way analysis of variance was used to compare the results for samples in the same group, and a paired *t*-test was used to compare samples collected at the same time.

Total protein from the midgut was extracted using the TCA/acetone method. The quantity was determined using the Pierce BCA Protein Assay Kit, and 3 μ g total protein was separated by 12% SDS-PAGE and transferred onto a nitrocellulose membrane using the electrode diverting method. According to the predicted sizes of CYP6B6 (58 kD), *β-Actin* (42 kD), and *HaADH5* (37 kD), the membrane was divided and tested using anti-CYP6B6 rabbit, anti-*β-Actin* mouse, and anti-*HaADH5* mouse polyclonal antiserum, respectively. The membrane was subsequently incubated with peroxidase-conjugated goat anti-mouse or anti-rabbit IgG and stained with a chemiluminescent substrate. The Western blotting results were quantified using Integrated Density (IntDen) measurement by grayscale analyses, with the *β-Actin* IntDen value

used for normalization of the target protein. The relative *HaADH5* and CYP6B6 IntDen values were analyzed by a paired *t*-test for samples from different groups collected at the same time.

Results

HaADH5 gene sequence analysis

The *HaADH5* cDNA sequence was amplified and assembled by 5'- and 3'-RACE to obtain the ORF. The 1128 bp *HaADH5* cDNA consisted of 38 bp 5'-UTR, 1005 bp ORF (from 39 to 1043), and 85 bp 3'-UTR (containing the polyadenylation signal ATTTAA). The ORF encoded a mature protein of 334 amino acids with a predicted molecular weight of 36.67 kD and a theoretical isoelectric point of 6.91. The *HaADH5* protein was conserved with most of the key residues for its function: 26 conserved residues important for interaction with nicotinamide adenine dinucleotide phosphate (P48, M129, T133, G154, G157, A158, V159, A178, G179, K183, Y198, N221, V222, C243, G244, S245, I246, S247, Y249, F276, L277, V278, I321, L322, G324, and N326) and five conserved residues important for substrate interaction (Y49, A52, C243, Y249, and W279) (Fig. 1).

A phylogenetic tree was constructed to assess the relationship of *HaADH5* with published ADHs from *Homo*, *Drosophila*, and *Bombyx* species (Fig. 2). *HaADH5* belonged to the class III of MDR-ADHs and tightly clustered together with the published ADH5 in *H. armigera* (GenBank accession number: AKD01727.1), with which it had 82% amino acid identity. The presently identified *HaADH5* has a disulfide bond (C142, C217) and five phosphorylation sites (Y49, Y57, Y61, S241, and S245), and it does not have an N-glycosylation site, signal peptide, or transmembrane helices. *HaADH5* structure prediction indicated homodimerization based on the homologous leukotriene B₄ 12-hydroxydehydrogenase/15-oxo-prostaglandin 13-reductase (LTB₄ 12-HD/PGR, PDB ID: 1v3u), which had 49.85% sequence identity. Its predicted structure contains 14 helices, 15 beta strands, five beta bulges, three beta sheets, 28 beta turns, three gamma turns forming three beta hairpins, seven helix-helix interactions, and five beta-alpha-beta units (Fig. 3). *HaADH5* homodimerization involves 11 hydrogen bonds and 146 non-bonded contacts of the dimer interface through 24 residues (E14, P17, K18, R19, A52, S55, R56, F237, V242, C243, G244, S245, S248, L266, V267, Q270, L271, K272, I273, E274, G275, F276, L277, and R280).

```

1      CAGTCGCCCCGCACACCGCGGAACGTAACACATCATAATGGTGAAGGCACGGAAATACG
1      M V K A R K Y
61     TCGTCAAAAAACACTTCGAAGGTTTACCAAAACGTGAAGATTTGAAAATAGTGAATACG
8      V V K K H F E G L P K R E D F E I V E Y
121    AGCTACCACCAATCAAGAATGGAGAGATTCTGTCAAAGTTGAGTGGGTGAGTGTGGATC
28     E L P P I K N G E I L V K V E W V S V D
181    CATACATGCGTGCCTACAATTCACGATACCCACACCGTACGACCAGTTTGGTTTCCAAG
48     P Y M R A Y N S R Y P T P Y D Q F G F Q
241    TCGGCTTGGTAGAAGATTCCAAGGACCCAGATATCCAGTTGGGACCAGAGTCGTCTCCC
68     V G L V E D S K D P R Y P V G T R V V S
301    ACAAAGGATGGTGTGACTATACTATCATCGATCCCAACGACAAAAATCCTGCTGCCGGG
88     H K G W C D Y T I I D P N D K N P A A G
361    AAGTGATAAGTTGCCGAACCTAAACGGTTTGTGCAATTCATTGGGAGTTGGCGCCGTGG
108    Q V Y K L P N L N G L S N S L G V G A V
421    GTATGCCTGGTGCACCGCTTACTTTGGATTTTTGGAAATTTGTCAGCCCAAAGCAGGTG
128    G M P G A T A Y F G F L E I C Q P K A G
481    AGACAGTGGTTGTGACGGGCGTCTGGAGCGGTCCGCTCGCTGGTCCGACAGATTGCTA
148    E T V V V T G A A G A V G S L V G Q I A
541    AGATCAAGGGCTGCAAGGTCATCGGCTTCGCTGGCTCTGACGATAAGGTGCAGTGGCTGG
168    K I K G C K V I G F A G S D D K V Q W L
601    AGGAGATCGGATTCGACAAGGCGATCAACTACAAGACTGTGACGTCTCCGCGGCGCTCA
188    E E I G F D K A I N Y K T A D V S A A L
661    AAGAAGCTGCTCCAAGGAGTCGATTGCTACTTCGACAATGTTGGCGGTGAGCTCAGCA
208    K E A A P K G V D C Y F D N V G G E L S
721    GTATCATTATCAACCAGATGAATGACTTCGGCAGGGTATCAGTTTGTGGCAGCATCAGTT
228    S I I I N Q M N D F G R V S V C G S I S
781    CATAACCGGATCCTGCAAACGTGCCAAGGCACCTATCTACAACCTGCTCTAGTGT
248    S Y N A D P A N V P K A P I L Q P A L V
841    TCAAACAATTGAAAATCGAAGGTTCTTGTGTGGCGTTGGATGAACCCAGTCGGAGG
268    F K Q L K I E G E L V W R W M N R Q S E
901    CACATACACAACCTTCAAGTGGATACAAAGTGGTCAGCTGAAGCCTAGAGAACATCA
288    A H T Q L I K W I Q S G Q L K P R E H I
961    CTGAAGGTTTCGAAAACATCTTCGATGCTTTTCTGGGAATATTGAACGGGAAAAATGTTG
308    T E G F E N I F D A F L G I L N G E N V
1021   GAAAGGCTGTTGTAATTATAAGTTTGTAAATCTACCTACTCAAGTTGATCCAAAGT
328    G K A V V K L *
1081   GTTGATCAGTGGCATTAAAGATCATGTTTATGTTGTAATAAAAAAAAAA

```

Fig. 1 The nucleotide and amino acid sequences of *HaADH5*. Conserved sites in *HaADH5* important for nicotinamide adenine dinucleotide phosphate (NADP) and substrate interaction are underlined and shaded, respectively. The dotted line indicates the poly(A) signal in the nucleotide sequence.

His-HaADH5 synthesis and purification

A highly expressed band over 45 kD was observed in the Transetta (pET32a-*HaADH5*) strain with 0.5 mmol/L IPTG induction at 20 °C for 4 h (released into the supernatant after gentle sonication); this band corresponded to the predicted size of the His-*HaADH5* fusion protein of 53.5 kD (Fig. 4A). The purification of His-*HaADH5* was performed by Ni²⁺ affinity chromatography at 4 °C. SDS-PAGE showed that His-*HaADH5* was well purified with only one band after the two steps with 200 mmol/L imidazole buffer (Fig. 4B). The amount of the fusion protein estimated by the protein BCA assay was 443.1 µg per 1 L LB induced culture, suggesting sufficient pro-

tein purification for activity determination. Testing of the purified fusion protein with anti-His tag monoclonal antibody (Fig. 4C) showed specific binding of anti-His tag to His-*HaADH5*, the size of which was slightly less than 55 kD.

Interaction between HaADH5 and the CYP6B6 promoter in vitro and in yeast

We investigated whether *HaADH5* protein could bind the HE1 element of the *CYP6B6* promoter using both *in vitro* and *in vivo* analyses (Fig. 5). Prokaryotically expressed *HaADH5* was used for the binding reaction

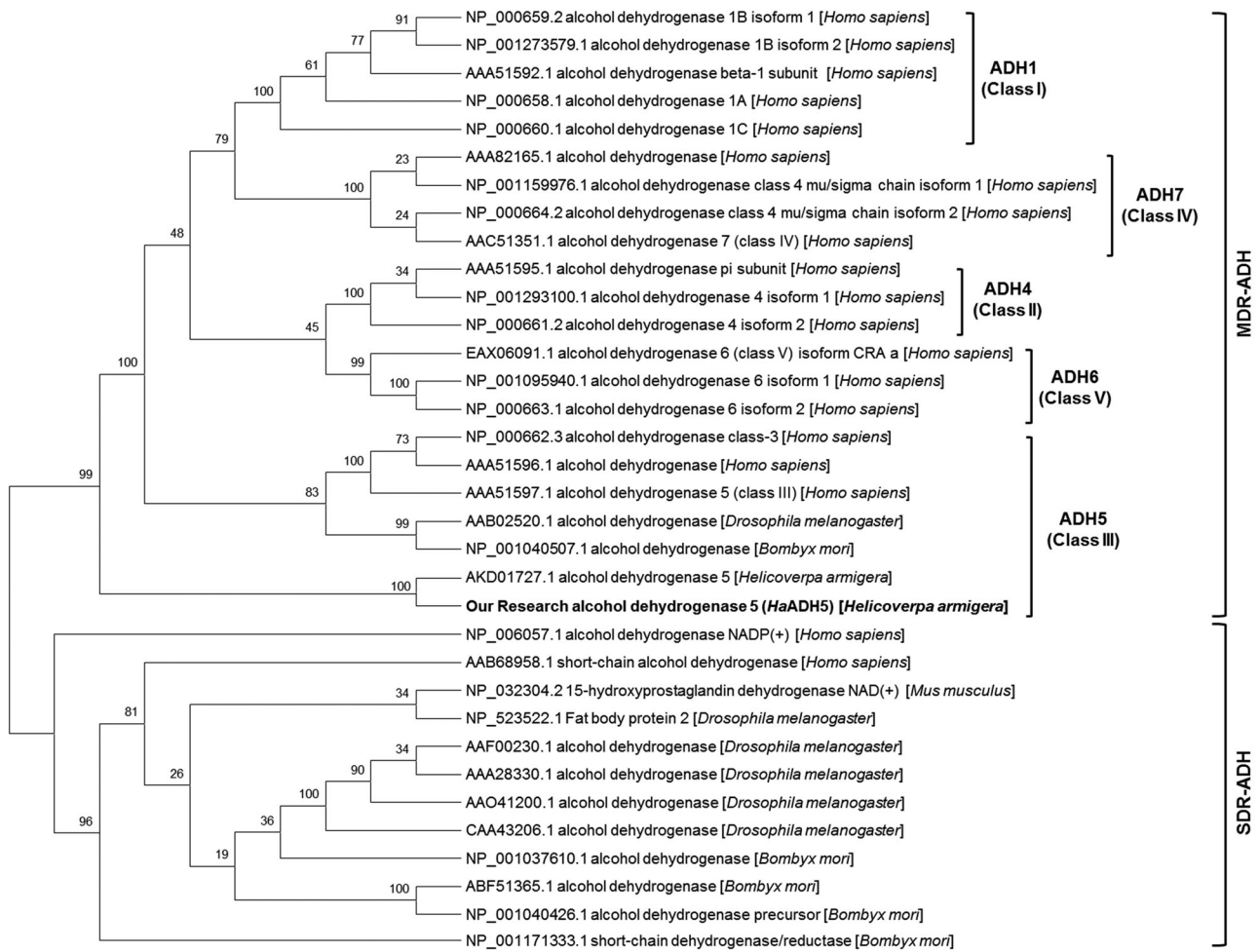


Fig. 2 Neighbor-joining tree of the *HaADH5* and published alcohol dehydrogenases (ADHs) from *Homo sapiens*, *Drosophila melanogaster*, *Bombyx mori*, and *Helicoverpa armigera*. MDR-ADH: medium-chain dehydrogenase/reductase family; SDR-ADH: short-chain dehydrogenase/reductase family.

with the HE1 probe by EMSA. Both 1 μ g and 2 μ g *HaADH5* protein led to a band shift in the positive test with HE1 probe (Fig. 5A). To confirm the DNA-binding activity of *HaADH5*, competition analyses were performed using unlabeled HE1 and an unrelated bHLH DNA fragment. The addition of excess unlabeled HE1 (lane 3) abolished the band shift; in contrast, the band shift was retained when the unrelated bHLH fragment was added (lane 4) (Fig. 5B). The results in Figure 5A and 5B show that *HaADH5* could bind to the HE1 element of *CYP6B6* *in vitro*. Transcription activity validation in yeast was also performed to test the interaction between *HaADH5* and the 2-TD responsive region of the *CYP6B6* promoter (Fig. 5C). The pGADT7-*HaADH5* plasmid was transformed into two reporter yeast strains,

Y1HGOLD (p4r-AbAi) and Y1HGOLD (p4m-AbAi), and these cells were coated onto SD/-Leu and SD/-Leu/AbA media. The transformed cells exhibiting normal growth on the SD/-Leu medium demonstrated that the whole process of transformation was feasible. For transformed Y1HGOLD (p4r-AbAi), there were four colonies on the SD/-Leu/AbA medium, whereas no growth was observed for the Y1HGOLD (p4m-AbAi) strain. Thus, on +AbA medium, the *AbA* gene was activated in the Y1HGOLD (p4r-AbAi) strain but not in the Y1HGOLD (p4m-AbAi) strain, indicating that *HaADH5* interacts with the *CYP6B6* promoter in yeast. Collectively, these results strongly suggest that *HaADH5* can bind to the HE1 element (2-TD responsive region) of the *CYP6B6* promoter in a sequence-specific manner.

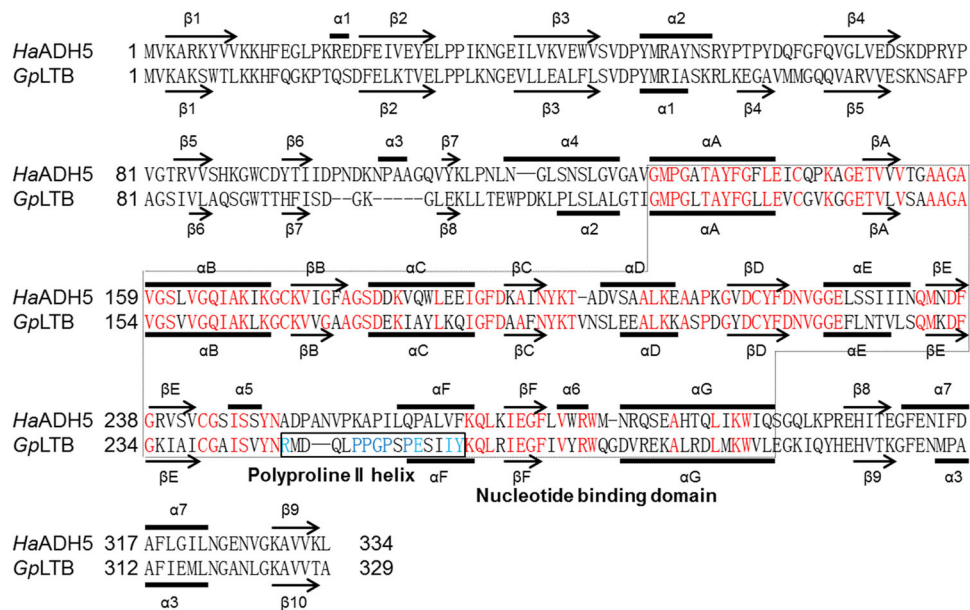


Fig. 3 Structure-based sequence alignment of *HaADH5* and *GpLTB*. *GpLTB*, guinea pig LTB_4 12-HD/PGR, Protein Data Bank identification code 1v3u. Secondary structural elements of *HaADH5* and *GpLTB* are indicated by arrows (β -strand) and bold lines (α -helix). The nucleotide-binding domain and the left-handed polyproline II helix region are surrounded by a thin dotted line and a thick solid line, respectively.

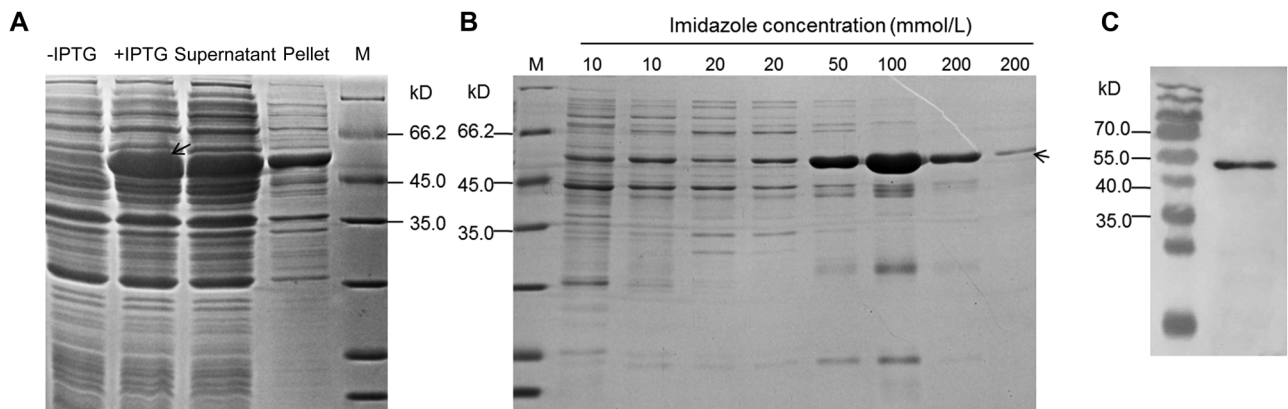


Fig. 4 The expression and purification of the His-*HaADH5* fusion protein. (A) Sodium dodecyl sulfate polyacrylamide gel electrophoresis (SDS-PAGE) for the protein products of the Transetta (pET32a-*HaADH5*) strain with isopropyl β -D-1-thiogalactopyranoside (IPTG) induction. (B) SDS-PAGE tracking the His-*HaADH5* protein purification progress. (C) Western blotting of the purified fusion protein with anti-His tag mouse monoclonal antibody.

HaADH5 and *CYP6B6* expression in the midgut of larvae exposed to 2-TD

To further investigate whether *HaADH5* can respond to 2-TD, we detected *HaADH5* expression in the midgut of 6th instar larvae treated with 10 mg/g 2-TD. Under treatment, *HaADH5* transcript levels significantly increased to the maximum level at 6 h ($P < 0.001$) and rapidly

returned to the normal level at 12 h ($P > 0.05$). The normal level was maintained until 30 h then decreased significantly to the minimum level at 48 h in the treatment group ($P < 0.001$). In light of the finding that *HaADH5* could bind to the *CYP6B6* promoter, *CYP6B6* expression was also monitored in response to 2-TD treatment. Its relative messenger RNA (mRNA) transcript levels were significantly increased at 6 h ($P < 0.001$) and reached

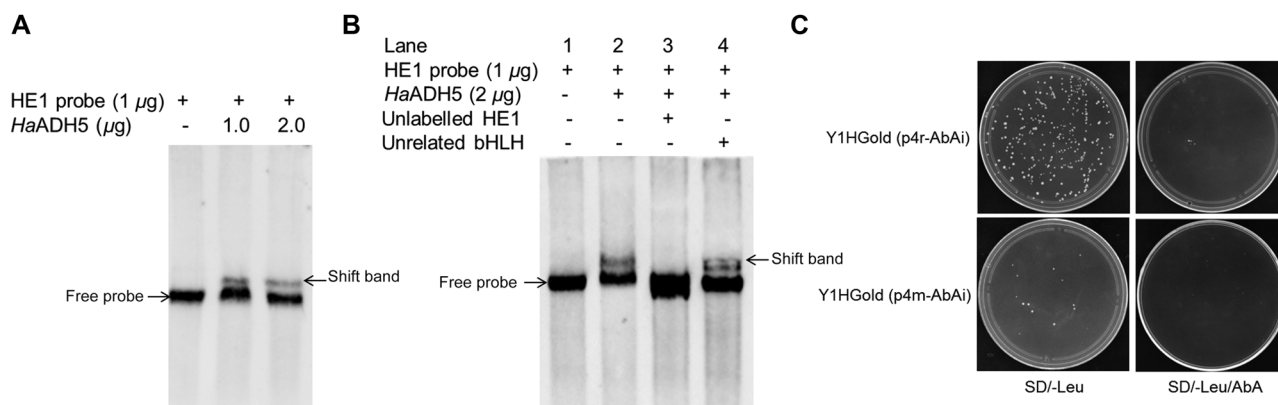


Fig. 5 Analysis of the interaction between *HaADH5* and the HE1 fragment of the *CYP6B6* promoter. (A) Interaction of the HE1 fragment and different amounts of *HaADH5* protein. (B) Electrophoretic mobility shift assay (EMSA) competition analysis of *HaADH5* and the HE1 fragment. Lane 1: negative control without protein; Lane 2: positive control with 2 µg protein; Lane 3: competition reaction with 2 µg protein and 200-fold unlabeled HE1 fragment; Lane 4: non-competition reaction with 2 µg protein and 200-fold unrelated bHLH fragment. (C) The interaction between *HaADH5* and the 2-tridecanone (2-TD) responsive region of the *CYP6B6* promoter in yeast.

the maximum level at 12 h ($P < 0.001$) under treatment. After a reduction to the normal level at 20 h, *CYP6B6* transcript levels decreased to the minimum level at 48 h ($P < 0.05$). Both transcripts of *HaADH5* and *CYP6B6* had significantly reduced expression at 48 h under 2-TD treatment (Fig. 6A).

Analysis of the relative amount of *HaADH5* protein indicated a significant increase at 12 and 20 h in the treatment group compared to the control group ($P < 0.05$) and a significant decrease at 48 h ($P < 0.01$). The relative amount of *CYP6B6* protein did not change at 12 h and 20 h in the treatment group, but it was significantly reduced at 48 h ($P < 0.05$). The relative amounts of *HaADH5* and *CYP6B6* protein were clearly reduced after 2-TD treatment for 48 h (Fig. 6B). Correlation analysis was subsequently performed for the relative amounts of *HaADH5* and *CYP6B6* protein with 2-TD treatment. The results indicated that the two proteins were positively correlated ($y = 0.1931x + 0.0981$, $R = 0.851$, $df = 3$) in the 10 mg/g treatment group.

Discussion

Insects and plants have complex and sophisticated mechanisms to adapt to each other during coevolution. To escape or survive from attacks by herbivorous insect, plants not only are equipped with physical carriers but also synthesize a kind of toxic defensive compound. On the other hand, herbivorous pests enhance the biological activity of certain detoxifying and metabolic enzymes to degrade these toxic substances for normal growth. Wild tomatoes rely on high concentration of 2-TD to resist the feeding of

several pests, such as *H. armigera*, *Aphis gossypii*, *Manduca sexta* and *Leptinotarsa decemlineata* (Gonçalves *et al.*, 1998; Lv *et al.*, 2012). 2-TD can stimulate ecdysone 20-monooxygenase activity in *Spodoptera frugiperda* and induce an enhanced level of tolerance to the carbamate insecticide carbaryl in *Heliothis zea* (Kennedy, 1984; Yu, 1995). Our published research showed that 2-TD treatment changed expression of *CYP6B6* in cotton bollworm and identified the 2-TD responsive element present in the *CYP6B6* promoter (Li *et al.*, 2014). And 2-TD was confirmed to suppress the 20-hydroxyecdysone (20E) titer and affect larval weight, pupation rate and adult emergence in cotton bollworm (Zhang *et al.*, 2016).

ADH5 is a central player in formaldehyde detoxification and S-nitrosoglutathione reduction to regulate oxidative stress, neuronal development, cardiovascular health, immune system balance, carcinogenesis, and single nucleotide polymorphisms (Lima *et al.*, 2009; Leung *et al.*, 2013; Blonder *et al.*, 2014). In this paper, we cloned a new *HaADH5* and found its expression significantly increased in a short time from the larval midgut of 10 mg/g 2-TD treated cotton bollworm. This result consists of the main function of insect ADH5 to work in the metabolism of endogenous compounds and toxic xenobiotics (Park & Kwak, 2009a; Huang *et al.*, 2016). In addition, ADH5 was suggested to be involved in metamorphosis process and mating stage in many *Lepidoptera* species (Li *et al.*, 2015; He *et al.*, 2017). Although ADH5 is not a typical transcription factor, previous studies showed that ADH5 also localizes to the nucleus and has a nucleotide-binding domain and a left-handed polyproline II helix region (Höög *et al.*, 2001; Hori *et al.*, 2004). In our study, the predicted

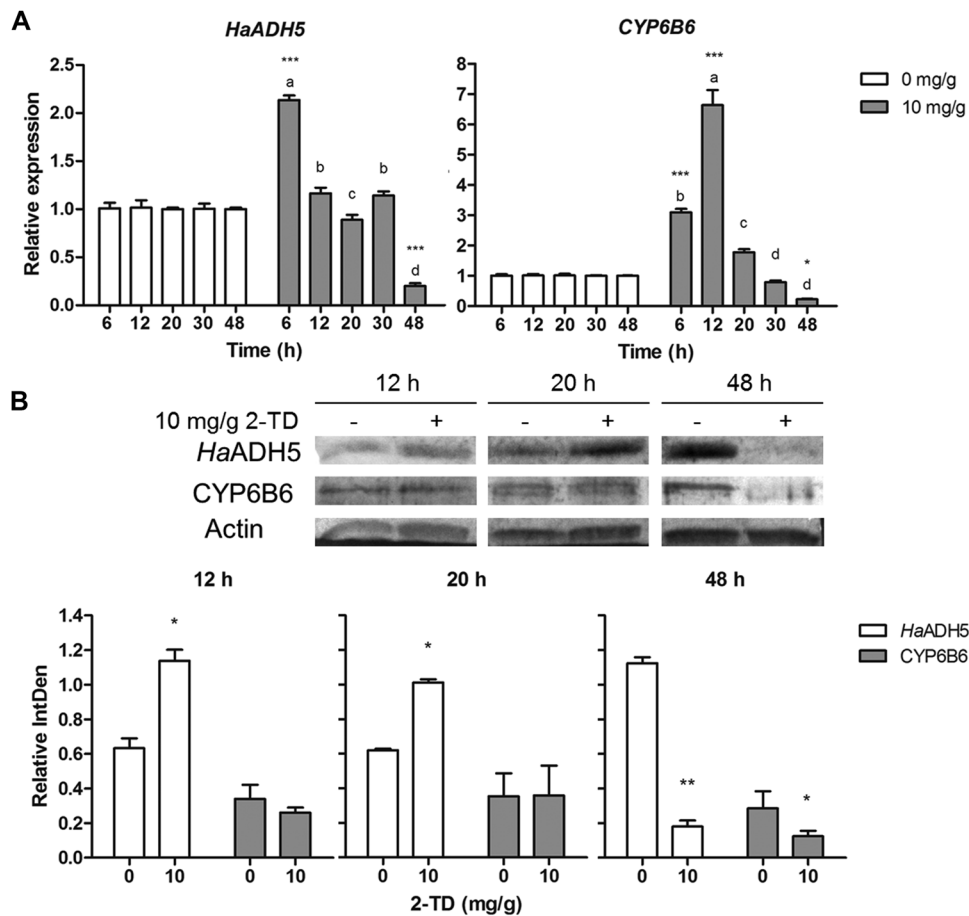


Fig. 6 The effect of 2-tridecanone (2-TD) on the expression of *HaADH5* and *CYP6B6* in the midgut of 6th instar larvae. (A) Relative expression of the target genes as indicated by messenger RNA transcript levels. (B) Relative amounts of protein. Different letters above the bars indicate significant differences between different time point samples under the same treatment condition ($P < 0.05$, one-way analysis of variance test). Asterisks indicate significant differences between the treatment and the control at the same time point ($*P < 0.05$, $**P < 0.01$, $***P < 0.001$, paired t -test).

structure of *HaADH5* was similar to that of *LTB₄12-HD/PGR* in terms of the presence of a nucleotide-binding domain. There were four prolines and a helix structure in the polyproline II helix region of *LTB₄12-HD/PGR*, corresponding to a proline percentage of 25%. Although the amino acids in this particular region were not conserved between *HaADH5* and *LTB₄12-HD/PGR*, *HaADH5* was also found to have a helix structure and four prolines, corresponding to 22.2% of the total amino acids in this region. Therefore, we suggest *HaADH5* may contribute to *CYP6B6* expression in response to 2-TD treatment to balance juvenile and ecdysis hormones and regulate the metamorphosis and development of *H. armigera*.

In this study, we found that *HaADH5* can bind to the 2-TD responsive element of the *CYP6B6* promoter both EMSA *in vitro* and transcription activity validation in

yeast. In addition to the new *HaADH5*, there is another published ADH5 in *H. armigera* (GenBank accession number: AKD01727.1). We also investigated whether the published ADH5 protein could bind to the *CYP6B6* promoter using the same methods. Both analyses indicated that it does not interact with the *CYP6B6* HE1 element (Fig. S1). Structure prediction of the published ADH5 protein indicated that it has 15 helices, 14 beta strands, 30 beta turns, and four gamma turns; however, it does not have a helix in the region homologous to the polyproline II helix of *LTB₄12-HD/PGR*, and it only has three prolines in this region, accounting for 16.6% of the total amino acids (data not shown). According to these results, the ability of the presently described *HaADH5* to bind and potentially regulate *CYP6B6* does not apply to the published ADH5 protein. This dissimilarity is also present among the three

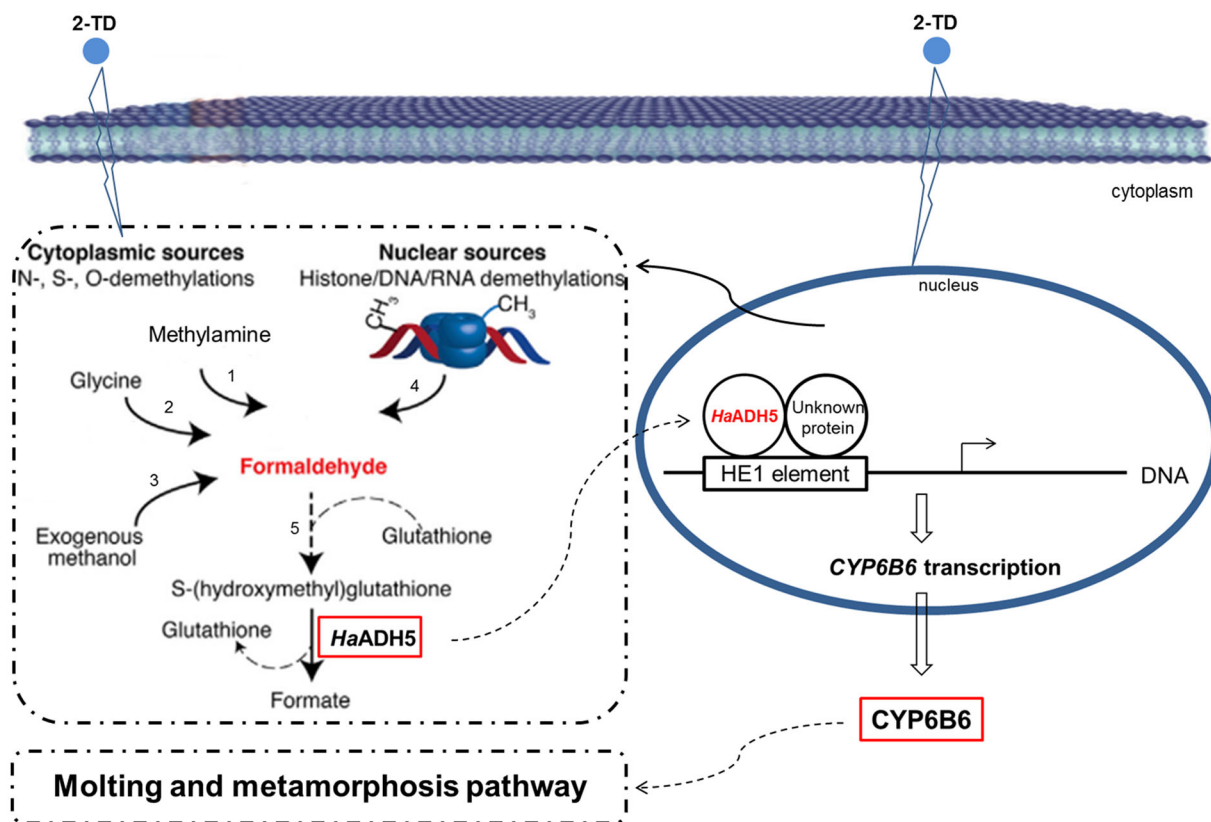


Fig. 7 The hypothesis pathway of *HaADH5* regulates *CYP6B6* expression to control growth and development in *Helicoverpa armigera* after 2-tridecanone (2-TD) treatment. The red font and box display the content of compound or protein was increased in the processes. 1: Semicarbazide-sentivite amine oxidase; 2: myeloperoxidase; 3: alcohol dehydrogenase 1 (ADH1) and catalase; 4: protein and nucleic acid demethylases; 5: spontaneous reaction.

isoforms of the transcription factor-like forkhead box A (FOXA) protein of *Homo sapiens* (FOXA1, FOXA2, and FOXA3), which each bind to slightly different nucleotide sequences (Tsai *et al.*, 2006).

After finding that *HaADH5* could interact with the 2-TD responsive region of the *CYP6B6* promoter, we wanted to know how *HaADH5* regulates the expression of *CYP6B6* in 6th larval midgut. Before this, we detected the *HaADH5* mRNA in all larval stages from the 1st to prepupa and four major tissues of 6th instar larvae including fat body, midgut, integument, and head. The result shows its mRNA existed in all tested samples, and the highest amount was in the prepupa and fat body (Fig. S2). The mRNA and protein of *ADH5* were highly expressed during various developmental stages from egg to adult in *C. riparius*, and in all the tested adult tissues including antennae, thoraxes, abdomens, legs and wings of *C. pomonella* (Park & Kwak, 2009a; Huang *et al.*, 2016). Moreover, the prepupa is a transition stage from larva to pupa; at this stage, tremendous changes in the concentration of

20-hydroxyecdysone and juvenile hormone regulate numerous differentially expressed genes for metamorphosis (Zhao *et al.*, 2006). The insect fat body is a central site for the organization of metabolic activity for growth and metamorphosis, and it contains many cell types that metamorphose upon hormone induction. The result of spatial and temporal expression further indicated *HaADH5* has an effect on the metamorphosis and development of *H. armigera*.

Then, we detected the expression of *HaADH5* and *CYP6B6* in 6th instar larvae in response to 2-TD treatment. *HaADH5* mRNA transcript levels increased the highest at 6 h and gradually decreased to the lowest at 48 h; similarly, *CYP6B6* transcripts peaked at 12 h and reached a minimum level at 48 h. There was a temporal order in the increase of transcription between *HaADH5* and *CYP6B6*. The *HaADH5* protein were significantly increased and *CYP6B6* protein did not change at 12 h and 20 h, while the two proteins were significantly reduced at 48 h and positively correlated in the treatment

group. According to these results, we propose that upon 2-TD treatment, overexpressed *HaADH5* can bind to the HE1 element to positively activate *CYP6B6* expression in a short timeframe.

Considering the influences of 2-TD treatment, functions of ADH5 and the ability of *HaADH5* to bind to the *CYP6B6* promoter, we further propose the hypothesis pathway about *HaADH5* regulates *CYP6B6* expression to control molting and metamorphosis when larvae are exposed to 2-TD in *H. armigera* (Fig. 7). First, kinds of precursors of formaldehyde are produced from cytoplasmic and nuclear sources by toxic 2-TD, and the expression of *HaADH5* is increased at the same time, then the catalyzed reactions of formaldehyde metabolism are enhanced and overexpress *HaADH5* actively or passively enter the nucleus. The *HaADH5* maybe form a dimerization transcript factor with an unknown protein and bind with the HE1 element of *CYP6B6* DNA. Subsequently, the transcription of *CYP6B6* is activated and increased in the nucleus, the overexpressed *CYP6B6* is released to cytoplasm and directly affect the downstream molting and metamorphosis processes. Surely, this hypothesis warrants further investigation using other methods in our next steps.

In conclusion, the present findings show that *HaADH5* could bind with the HE1 element of *CYP6B6* promoter and activate *CYP6B6* transcription in response to 2-TD treatment. Therefore, *HaADH5* could potentially be used as a molecular marker to study detoxification mechanisms triggered by exogenous substances and also as a molecular target to control the growth and development of cotton bollworm.

Acknowledgments

This work was supported by the National Natural Science Foundation of China (31471781), Natural Science Foundation of Xinjiang Region in China (2016D01C042) and Tianshan Cedar Project in 2017 (2017xs20).

Disclosure

The authors have no conflict of interest, including specific financial interests and relationships and affiliations relevant to the subject of this manuscript.

References

- Ai, X.Y., Zhao, J., Wang, Y.M., Wei, Y.J. and Liu, X.N. (2017) Optimization of prokaryotic expression of soluble alcohol dehydrogenase from *Helicoverpa armigera*. *Biotechnology*, 27(1), 65–70.
- Anand, P., Hausladen, A., Wang, Y.J., Zhang, G.F., Stomberski, C., Brunengraber, H. *et al.* (2014) Identification of S-nitroso-CoA reductases that regulate protein S-nitrosylation. *Proceedings of the National Academy of Science USA*, 111(52), 18572–18577.
- Blonder, J.P., Mutka, S.C., Sun, X.C., Qiu, J., Green, L.H., Mehra, N.K. *et al.* (2014) Pharmacologic inhibition of S-nitrosogluthione reductase protects against experimental asthma in BALB/c mice through attenuation of both bronchoconstriction and inflammation. *Pulmonary Medicine*, 14, 3.
- Burgos, B.G., Wit, N., Meiser, J., Dingler, F.A., Pietzke, M., Mulderig, L. *et al.* (2017) Mammals divert endogenous genotoxic formaldehyde into one-carbon metabolism. *Nature*, 548, 549–554.
- Chandra Sharath, G., Asokan, R., Manamohan, M., Kumar, K.N. and Sita, T. (2014) Evaluation of reference genes for quantitative real-time PCR normalization in cotton bollworm, *Helicoverpa armigera*. *Molecular Biology (Mosk)*, 48, 927–938.
- Chase, J.R., Poolman, M.G. and Fell, D.A. (2009) Contribution of NADH increases to ethanol's inhibition of retinol oxidation by human ADH isoforms. *Alcoholism: Clinical and Experimental Research*, 33, 571–580.
- Corti, A., Franzini, M., Scataglini, I. and Pompella, A. (2014) Mechanisms and targets of the modulatory action of S-nitrosogluthione (GSNO) on inflammatory cytokines expression. *Archives of Biochemistry and Biophysics*, 562, 80–91.
- Danielsson, O., Atrian, S., Luque, T., Hjelmqvist, L., González, D.R. and Jörnvall, H. (1994) Fundamental molecular differences between alcohol dehydrogenase classes. *Proceedings of the National Academy of Sciences USA*, 91, 4980–4984.
- Deltour, L., Foglio, M.H. and Duester, G. (1999) Metabolic deficiencies in alcohol dehydrogenase *Adh1*, *Adh3*, and *Adh4* null mutant mice. *Journal of Biological Chemistry*, 274, 16796–16801.
- Fernández, M.R., Biosca, J.A. and Parés, X. (2003) S-nitrosogluthione reductase activity of human and yeast glutathione-dependent formaldehyde dehydrogenase and its nuclear and cytoplasmic localisation. *Cellular and Molecular Life Sciences*, 60, 1013–1018.
- Gonçalves, M.I.F., Maluf, W.R., Gomes, L.A.A. and Barbosa, L.V. (1998) Variation of 2-tridecanone level in tomato plant leaflets and resistance to two mite species (*Tetranychus* sp.). *Euphytica*, 104, 33–38.
- Gu, S.H., Wu, K.M., Guo, Y.Y., Pickett, J.A., Field, L.M., Zhou, J.J. *et al.* (2013) Identification of genes expressed in the sex pheromone gland of the black cutworm *Agrotis ipsilon* with putative roles in sex pheromone biosynthesis and transport. *BMC Genomics*, 14:636.

- He, P., Zhang, Y.F., Hong, D.Y., Wang, J., Wang, X.L., Zuo, L.H. *et al.* (2017) A reference gene set for sex pheromone biosynthesis and degradation genes from the diamondback moth, *Plutella xylostella*, based on genome and transcriptome digital gene expression analyses. *BMC Genomics*, 18: 219.
- Hess, D.T., Matsumoto, A., Kim, S.O., Marshall, H.E. and Stamler, J.S. (2005) Protein S-nitrosylation: Purview and parameters. *Nature Reviews Molecular Cell Biology*, 6, 150–166.
- Höög, J.O., Hedberg, J.J., Strömberg, P. and Svensson, S. (2001) Mammalian alcohol dehydrogenase-functional and structural implications. *Journal Biomedical Science*, 8, 71–76.
- Hori, T., Yokomizo, T., Ago, H., Sugahara, M., Ueno, G., Yamamoto, M. *et al.* (2004) Structural basis of leukotriene B₄ 12-hydroxydehydrogenase/15-Oxo-prostaglandin 13-reductase catalytic mechanism and a possible Src homology 3 domain binding loop. *The Journal of Biological Chemistry*, 279, 22615–22623.
- Huang, L.N., Cheng, T.T., Wang, X.H., Wei, Y.J., Zhao, J., Li, J.Y. *et al.* (2015) The cloning, expression and preparation of polyclonal antibody of β -actin gene from *Helicoverpa armigera*. *Biotechnology Bulletin*, 31(12), 138–145.
- Huang, X.L., Liu, L., Su, X.J. and Feng, J.N. (2016) Identification of biotransformation enzymes in the antennae of codling moth *Cydia pomonella*. *Gene*, 580, 73–79.
- Jensen, D.E., Belka, G.K. and DuBois, G.C. (1998) S-Nitrosoglutathione is a substrate for rat alcohol dehydrogenase class III isoenzyme. *Biochemical Journal*, 331, 659–668.
- Kaiser, R., Holmquist, B., Hempel, J., Vallee, B.L. and Jörnvall, H. (1988) Class III human liver alcohol dehydrogenase: a novel structural type equidistantly related to the class I and class II enzymes. *Biochemistry*, 27, 1132–1140.
- Kawanishi, M., Matsuda, T. and Yag, T. (2014) Genotoxicity of formaldehyde: molecular basis of DNA damage and mutation. *Frontiers in Environmental Science*, 2, 1–8.
- Kennedy, G.G. (1984) 2-tridecanone, tomatoes and *Heliothis zea*: potential incompatibility of plant antibiosis with insecticidal control. *Entomologia Experimentalis et Applicata*, 35, 305–311.
- Koivusalo, M., Baumann, M. and Uotila, L. (1989) Evidence for the identity of glutathione-dependent formaldehyde dehydrogenase and class III alcohol dehydrogenase. *FEBS Letters*, 257, 105–109.
- Li, F., Liu, X.N., Zhu, Y., Ma, J., Liu, N. and Yang, J.H. (2014) Identification of the 2-tridecanone responsive region in the promoter of cytochrome P450 *CYP6B6* of the cotton bollworm, *Helicoverpa armigera* (Lepidoptera: Noctuidae). *Bulletin of Entomological Research*, 104, 801–808.
- Li, Z.Q., Zhang, S., Luo, J.Y., Wang, C.Y., Lv, L.M., Dong, S.L. *et al.* (2015) Transcriptome comparison of the sex pheromone glands from two sibling *Helicoverpa* species with opposite sex pheromone components. *Scientific Reports*, <https://doi.org/10.1038/srep09324>.
- Lima, B., Lam, G.K.W., Xie, L., Diesen, D.L., Vilamizar, N., Nienaber, J. *et al.* (2009) Endogenous S-nitrosothiols protect against myocardial injury. *Proceedings of the National Academy of Sciences USA*, 106, 6297–6302.
- Liu, X.N., Liang, P., Gao, X.W. and Shi, X.Y. (2006) Induction of the cytochrome P450 activity by plant allelochemicals in the cotton bollworm, *Helicoverpa armigera* (Hübner). *Pesticide Biochemistry and Physiology*, 84, 127–134.
- Leung, J., Wei, W. and Liu, L. (2013) S-nitrosoglutathione reductase deficiency increases mutagenesis from alkylation in mouse liver. *Carcinogenesis*, 34, 984–989.
- Luo, X.G., Kranzler, H.R., Zuo, L.J., Zhang, H.P., Wang, S. and Gelernter, J. (2008) ADH7 variation modulates extraversion and conscientiousness in substance dependent subjects. *American Journal of Medical Genetics. Part B, Neuropsychiatric Genetics*, 147, 179–186.
- Lv, M., Sun, H.H., Wang, L.H. and Gao, X.W. (2012) Effects of secondary metabolites on activities of glutathione S-transferases, carboxylesterase in aphid. *Chinese Agricultural Science Bulletin*, 28, 253–256.
- Martínez, R.A., Cadenas, S. and Lamas, S. (2011) Nitric oxide signaling: classical, less classical, and nonclassical mechanisms. *Free Radical Biology and Medicine*, 51, 17–29.
- Oscar, B.M. and Marinkovic, K. (2003) Alcoholism and the brain: an overview. *Alcohol Research and Health*, 27, 125–133.
- Östberg, L.J., Persson, B. and Höög, J.O. (2016) Computational studies of human class V alcohol dehydrogenase—the odd sibling. *BMC Biochemistry*, 17: 16.
- Ou, J., Deng, H.M., Zheng, S.C., Huang, L.H., Feng, Q.L. and Liu, L. (2014) Transcriptomic analysis of developmental features of *Bombyx mori* wing disc during metamorphosis. *BMC Genomics*, 15(1): 820.
- Park, K. and Kwak, I.S. (2009a) Alcohol dehydrogenase gene expression in *Chironomus riparius* exposed to di(2-ethylhexyl) phthalate. *Comparative Biochemistry and Physiology*, 150, 361–367.
- Park, K. and Kwak, I.S. (2009b) Characterization and expression of *Chironomus riparius* alcohol dehydrogenase gene under heavy metal stress. *Environmental Health and Toxicology*, 24, 107–117.
- Pontel, L.B., Rosado, I.V., Burgos, B.G., Garaycochea, J.I., Yu, R., Arends, M.J. *et al.* (2015) Endogenous formaldehyde is a hematopoietic stem cell genotoxin and metabolic carcinogen. *Molecular Cell*, 60, 177–188.
- Ramchandani, V.A., Bosron, W.F. and Li, T.K. (2001) Research advances in ethanol metabolism. *Pathologie Biologie*, 49, 676–682.
- Shakeel, M., Zhu, X., Kang, T.H., Wan, H. and Li, J.H. (2015) Selection and evaluation of reference genes for quantitative gene expression studies in cotton bollworm, *Helicoverpa armigera*

- (Lepidoptera: Noctuidae). *Journal of Asia-Pacific Entomology*, 18, 123–130.
- Smith, B.C. and Marletta, M.A. (2012) Mechanisms of S-nitrosylthiol formation and selectivity in nitric oxide signaling. *Current Opinion in Chemical Biology*, 16, 498–506.
- Tibbetts, A.S. and Appling, D.R. (2010) Compartmentalization of mammalian folate-mediated one-carbon metabolism. *Annual Review of Nutrition*, 30, 57–81.
- Tsai, K.L., Huang, C.Y., Chang, C.H., Sun, Y.J., Chuang, W.J. and Hsiao, C.D. (2006) Crystal structure of the human FOXK1a-DNA complex and its implications on the diverse binding specificity of winged helix/forkhead proteins. *The Journal of Biological Chemistry*, 281(25), 17400–17409.
- Vandesompele, J., De Preter, K., Pattyn, F., Poppe, B., Van Roy, N., De Paepe, A. et al. (2002) Accurate normalization of real-time quantitative RT-PCR data by geometric averaging of multiple internal control genes. *Genome Biology*, 3(7), research0034.1-0034.11.
- Vogel, H., Heidel, A.J., Heckel, D.G. and Groot, A.T. (2010) Transcriptome analysis of the sex pheromone gland of the noctuid moth *Heliothis virescens*. *BMC Genomics*, 11, 1–21.
- Wei, W., Li, B., Hanes, M.A., Kakar, S., Chen, X. and Liu, L.M. (2010) S-nitrosylation from GSNOR deficiency impairs DNA repair and promotes hepatocarcinogenesis. *Science Translational Medicine*, 2(19): 19ra13.
- Wei, Y.J., Zhang, L., Cheng, T.T., Ma, J. and Liu, X.N. (2015) Preparation of the polyclonal antibody against P450 *CYP6B6* from *Helicoverpa armigera*. *Life Science Research*, 19(6), 497–500.
- Yang, Z.N., Bosron, W.F. and Hurley, T.D. (1997) Structure of human chi chi alcohol dehydrogenase: a glutathione-dependent formaldehyde dehydrogenase. *Journal of Molecular Biology*, 265, 330–343.
- Yu, C.H., Gao, X.W. and Zheng, B.Z. (2002) Induction of the cytochrome P450 by 2-tridecanone in *Helicoverpa armigera*. *Acta Entomologica Sinica*, 45, 1–7.
- Yu, S.J. (1995) Allelochemical stimulation of ecdysone 20-monooxygenase in fall armyworm larvae. *Archives Insect Biochemistry and Physiology*, 28, 365–375.
- Zhang, L., Lu, Y., Xiang, M., Shang, Q.L. and Gao, X.W. (2016) The retardant effect of 2-tridecanone, mediated by cytochrome P450, on the development of cotton bollworm, *Helicoverpa armigera*. *BMC Genomics*, 17, 954.
- Zhao, J., Liu, N., Ma, J., Huang, L.N. and Liu, X.N. (2016a) Effect of silencing *CYP6B6* of *Helicoverpa armigera* (Lepidoptera: Noctuidae) on its growth, development, and insecticide tolerance. *Journal of Economic Entomology*, 109(6), 2506–2516.
- Zhao, J., Liu, X.N., Li, F., Zhuang, S.Z., Huang, L.N., Ma, J. et al. (2016b) Yeast one-hybrid screening the potential regulator of *CYP6B6* overexpression of *Helicoverpa armigera* under 2-tridecanone stress. *Bulletin of Entomological Research*, 106, 182–190.
- Zhao, X.F., He, H.J., Dong, D.J. and Wang, J.X. (2006) Identification of differentially expressed proteins during larval molting of *Helicoverpa armigera*. *Journal of Proteome Research*, 5, 164–169.

Manuscript received May 15, 2019

Final version received August 13, 2019

Accepted August 19, 2019

Supporting Information

Additional supporting information may be found online in the Supporting Information section at the end of the article.

Fig. S1. The interaction between the published ADH5 and HE1 fragment of *CYP6B6* promoter.

Fig. S2. The temporal and spatial expression profile of the *HaADH5* in *H. armigera*.